arXiv:1210.0488v1 [quant-ph] 1 Oct 2012

Phonon-mediated population inversion in a semiconductor quantum-dot cavity system

S. Hughes*
Department of Physics, Queen's University, Kingston, Ontario, Canada K7L 3N6

H. J. Carmichael
Department of Physics, University of Auckland, Private Bag 92019, Auckland, New Zealand

Achieving population inversion in solid-state two-level systems like quantum dots in semiconductor cavities could lead to fundamentally new regimes of light-matter interaction and the development of miniaturized non-classical light sources at telecom frequencies. Here we show that phonon-induced scattering between a driven cavity mode and a quantum dot can promote the exciton to a regime of pronounced steady-state population inversion. Using a polaron-based master equation, we demonstrate excited-state populations above 0.9 in an InAs dot at a phonon bath temperature of 4 K. The mechanism of inversion is phonon-mediated switching between ground- and excited-state branches of the multi-photon ladder of states. Quantum trajectory simulations extend this qualitative interpretation to a quantitatively realistic model.

The ability to achieve inversion and lasing in atomic and solid state systems is a topic of continuing interest [1]. Recently, in the domain of cavity-QED, regimes of "single atom lasing" and non-classical light emission have been studied [2, 3]. According to the common wisdom, schemes to achieve population inversion must exploit a multi-level manifold of material states; inversion (in the steady state) is not possible for a driven two-level system (TLS). The wisdom is restricted to a TLS coupled to classical fields only and a non-engineered environment, however. When interacting with a *quantized* radiation mode, a TLS may be inverted by two-photon excitation of higher lying levels of the quantized *matter plus field* [4–6]. A TLS in interaction with an environment near a photonic bandgap may also be inverted, by way of an asymmetry of the Mollow triplet [7]; very high (many orders of magnitude) contrast in the sideband decay rates is required, though.

In contrast to atoms, unique features of semiconductor quantum dot (QDs) include their large optical dipole moments and engineerable emission wavelength; other attractive features are the fixed QD position and ability to integrate with cavities and waveguides using standard semiconductor fabrication techniques [8]. Semiconductor QDs differ from atoms at a more fundamental level, however, and call for extra care when describing the quantum light-matter interaction. In particular, QDs are typically embedded in a solid state lattice where electron-phonon interactions, though often ignored, are known to impact optical properties, affecting photoluminescence lineshapes [9], coherent Rabi oscillation [10], and the Mollow triplet spectrum of resonance fluorescence [11, 12]. Phonon-mediated scattering can cause excitation-induced dephasing [10, 13] which is detrimental to the exploitation of quantum optical interactions. An intriguing question is thus: what impact does electron-phonon scattering have when one tries to coherently drive an excitonic transition coupled to a quantized radiation mode into the regime of population inversion? Here we find a surprising result. We find that contrary to it being detrimental, acoustic-phonon-mediated scattering can be exploited to achieve significant exciton inversion via a mechanism entirely different to previously proposed schemes for inverting a TLS. The mechanism is richer and significantly more efficient. It relies on the natural asymmetry between phonon emission and absorption at low bath temperatures, exploiting a phonon-assisted one-way coupling (scattering) between the exciton and the cavity mode when the cavity is blue detuned with respect to the zero phonon line (ZPL).

In this Letter we propose and characterize the photon-assisted scheme using a semiconductor quantum-optics formalism that includes phonon interactions by way of an effective master equation (ME) [14]. The ME takes electron-acoustic-phonon interactions into account at a microscopic level using a polaron transform [12, 14], and introduces cavity and QD decay at the level of a Lindblad description. We consider a single QD embedded within a small high Q dielectric cavity, as shown schematically in Figs. 1(a) and 1(b). The cavity mode is subject to coherent cw pumping (η_c in the figure). The advantage of cavity over exciton pumping is that it mitigates problems with excitation-induced dephasing [11, 14], a process that accompanies excitation via the exciton-phonon reservoir [11, 12]; it also allows for pumping through a waveguide input channel [15] [cf. Fig. 1(b)].

Theory.—We work in a frame rotating at the laser pump frequency ω_L. The Hamiltonian, excluding QD and cavity decay, is

$$\begin{aligned} H \; &= \; \hbar\Delta_{xL}\sigma^+\sigma^- + \hbar\Delta_{cL}a^\dagger a + \hbar g(\sigma^+ a + a^\dagger\sigma^-) + H^c_{\rm drive} \\ &\quad + \sigma^+\sigma^- \sum_q \hbar\lambda_q(b_q + b_q^\dagger) + \sum_q \hbar\omega_q b_q^\dagger b_q \, , \end{aligned} \tag{1}$$

where $b_q^\dagger$ and b_q are the phonon creation and annihilation operators of mode q of the bath, $a^\dagger$ and a are the photon creation and annihilation operators of the cavity mode, and σ^+ and σ^- are Pauli raising and lowering operators

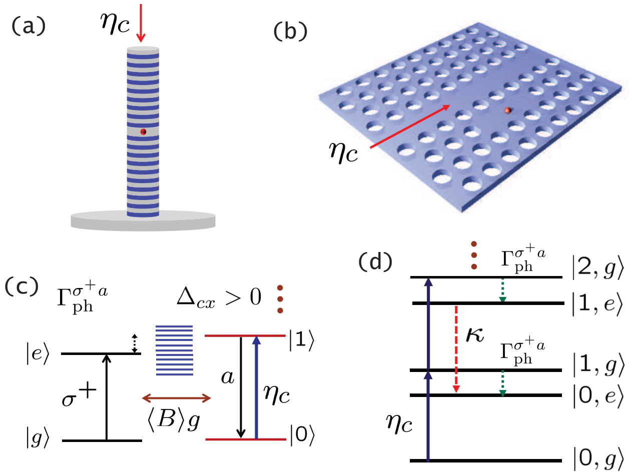

FIG. 1: (Color online) (a-b) Schematics of two example semiconductor cavity-QED systems with coherent cavity drive η_c. (c) Exciton energy levels ($|e\rangle$ and $|g\rangle$) and first two levels of the cavity ladder ($|0\rangle$ and $|1\rangle$), with exciton coupling to a phonon bath; $\langle B\rangle g$ and $\Gamma_{\rm ph}^{\sigma^+}$ effect phonon-induced coupling between the exciton and cavity (see text); Δ_{cx} is the cavity-exciton detuning. (d) Simplified level scheme showing the approximate system behavior as ground- and excited-state harmonic oscillators with one-way coupling through phonon-mediated scattering (coherent coupling $\langle B\rangle g$ omitted); κ is the cavity decay rate.

for the exciton (electron-hole pair); $\Delta_{\alpha L} \equiv \omega_\alpha - \omega_L$ ($\alpha = x, c$) designates the exciton (frequency ω_x) and cavity (frequency ω_c) detuning from ω_L, and the Hamiltonian of the cavity drive is $H^c_{\rm drive} = \hbar\eta_c(a + a^\dagger)$.

To move from Hamiltonian (1) to the effective ME, one first transforms to a polaron frame, which formally recovers the independent boson model [16–18]; this model is known to describe the characteristic spectrum of an exciton coupled to a phonon bath [9]. From here the derived ME [12, 17, 19] treats coherent electron-phonon coupling nonperturbatively through a mean phonon displacement,

$$\langle B\rangle = \exp\left[-\frac{1}{2}\int_0^\infty d\omega \frac{J(\omega)}{\omega^2}\coth(\hbar\omega/2k_bT)\right], \tag{2}$$

with $J(\omega)$ the phonon spectral function, and scattering in the second-order Born approximation (see Refs. [12, 14] for details). With the addition of QD and cavity decay, the time-convolutionless ME for the reduced density operator is:

$$\frac{\partial\rho}{\partial t} = \frac{1}{i\hbar}[H'_S, \rho] + \mathcal{L}_{\rm ph}\rho + \mathcal{L}\rho, \tag{3}$$

with polaron-transformed system Hamiltonian

$$H'_S = \hbar(\Delta_{xL} - \Delta_P)\sigma^+\sigma^- + \hbar\Delta_{cL}a^\dagger a + \hbar g' X_g + H^c_{\rm drive}, \tag{4}$$

with polaron shift $\Delta_P = \int_0^\infty d\omega J(\omega)/\omega$ (absorbed into the exciton frequency below) and $g' = \langle B\rangle g$, and the phonon scattering term

$$\mathcal{L}_{\rm ph}\rho = -g'^2 \sum_{m=g,u}\int_0^\infty d\tau G_m(\tau)[X_m, X_m(\tau)\rho] + \text{H.c.}, \tag{5}$$

where $X_m(\tau) = e^{-iH'_S\tau/\hbar}X_m e^{iH'_S\tau/\hbar}$, with $(X_g, iX_u) = a^\dagger\sigma^- \pm \sigma^+ a$, and $G_g(t) = \cosh[\phi(t)] - 1$ and $G_u(t) = \sinh[\phi(t)]$ are the polaron Green functions [16, 17], with

$$\phi(t) = \int_0^\infty d\omega \frac{J(\omega)}{\omega^2}\left[\coth(\hbar\omega/2k_bT)\cos(\omega t) - i\sin(\omega t)\right]. \tag{6}$$

For the phonon spectral function we adopt the form $J(\omega) = \alpha_p\omega^3\exp(-\omega^2/2\omega_b^2)$, which describes the electron-acoustic-phonon interaction via a deformation potential interaction, the dominant source of phonon scattering for InAs and GasAs QDs [21]. The last term on the right-hand side of Eq. (3) is a sum of three Lindblads: $\mathcal{L} = \kappa\mathcal{L}[a] + (\gamma/2)\mathcal{L}[\sigma^-] + \gamma'\mathcal{L}[\sigma_{ee}]$, where $\mathcal{L}[\xi]\rho = 2\xi\rho\xi^\dagger - \xi^\dagger\xi\rho - \rho\xi^\dagger\xi$ and $\sigma_{ee} = |e\rangle\langle e|$. It accounts for cavity decay at rate 2κ, exciton decay at rate γ, and pure dephasing of the exciton at rate γ'; these processes broaden the ZPL.

The full form of the outlined model yields an involved solution scheme and little physical insight. We therefore turn to an effective Lindblad ME, which is shown by Roy and Hughes [14] to yield solutions in very good agreement with Eq. (3). For cavity excitation it makes the replacement:

$$\mathcal{L}_{\rm ph}\rho \rightarrow \frac{\Gamma_{\rm ph}^{\sigma^+a}}{2}\mathcal{L}[\sigma^+a]\rho + \frac{\Gamma_{\rm ph}^{a^\dagger\sigma^-}}{2}\mathcal{L}[a^\dagger\sigma^-]\rho, \tag{7}$$

with scattering rates

$$\Gamma_{\rm ph}^{\sigma^+a/a^\dagger\sigma^-} = 2g'^2\,\mathrm{Re}\left[\int_0^\infty d\tau\, e^{\pm i\Delta_{cx}\tau}\left(e^{\phi(\tau)} - 1\right)\right], \tag{8}$$

where $\Delta_{cx} = \omega_c - \omega_x$ is the cavity-exciton detuning. In this prescription, phonon scattering amounts to a one-way coupling between the driven cavity mode and QD exciton expressed through quantum jumps. There are jumps in two directions—photon creation accompanied by exciton deexitation (rate $\Gamma_{\rm ph}^{a^\dagger\sigma^-}$) and photon annihilation accompanied by excitation of the exciton (rate $\Gamma_{\rm ph}^{\sigma^+a}$)—though Eqs. (6) and (8) yield an asymmetry of rates. The asymmetric scattering rates allow for phonon-mediated inversion.

The results which follow are obtained by solving ME (3) numerically with electron-phonon scattering treated in the Lindblad approximation [Eq. (7)]. As depicted in Fig. 1(c), we adopt a basis of truncated photon states, $|n\rangle$, $n = 1, \ldots, N$, and the two exciton states, $|g\rangle$ and $|e\rangle$. We find that $N = 50$ is required for convergence at the chosen pump levels, especially in the presence of electron-phonon scattering. For a simplest picture of the

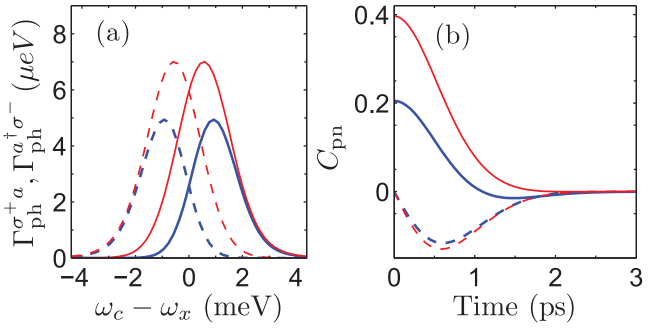

FIG. 2: (Color online) (a) Rates $\Gamma_{\rm ph}^{\sigma^+a}$ (solid) and $\Gamma_{\rm ph}^{a^\dagger\sigma^-}$ (dashed) as a function of cavity detuning from the zero phonon line; for an effective cavity-exciton coupling rate $g' = 0.1\,$meV, phonon spectral parameters $\omega_b = 1\,$meV and $\alpha_p/(2\pi)^2 = 0.06\,$ps^2, and bath temperatures $T = 4\,$K (blue, thicker curves) and $T = 10\,$K (red, thinner curves). (b) Corresponding phonon correlation function, $C_{\rm pn}(t) = \exp[\phi(t)] - 1$, with showing real (solid) and imaginary parts (dashed).

inversion mechanism, Fig. 1(d) shows the two harmonic oscillator ladders, coordinated with $|g\rangle$ and $|e\rangle$, which result when the Jaynes-Cummings (JC) interaction term ($\hbar g' X_g$) is dropped from the polaron-transformed Hamiltonian. With this simplification, if the cavity is detuned to the blue of the zero-photon line, as shown, $\Gamma_{\rm ph}^{\sigma^+a}$ may dominate over $\Gamma_{\rm ph}^{\sigma^+a}$ to pump the exciton into its excited state.

Results.—We choose material parameters suitable for InAs QDs, with $\omega_b = 1\,$meV and $\alpha_p/(2\pi)^2 = 0.06\,$ps^2 [12, 20], and consider a QD-cavity system in the strong coupling regime of cavity QED, with $g' = 100\,\mu$eV, $\gamma = 1\,\mu$eV, $\kappa = 50\,\mu$eV, and $\gamma' = 4\,\mu$eV. These numbers are consistent with various QD-cavity experiments. To gain insight into the relevant phonon scattering rates, we plot them as a function of cavity-exciton detuning for two different bath temperatures in Fig. 2(a). The figure highlights the mentioned asymmetry between $\Gamma_{\rm ph}^{\sigma^+a}$ and $\Gamma_{\rm ph}^{a^\dagger\sigma^-}$, more pronounced at the lower temperature of 4 K than 10 K (where the process of phonon absorption is less likely). Note also that the scattering rates at 10 K are larger than at 4 K, even though $\langle B\rangle\,(10\,{\rm K}) = 0.84$ is lower than $\langle B\rangle\,(4\,{\rm K}) = 0.91$. In Fig. 2(b), we also plot the phonon correlation function, $C_{\rm pn}(t) \equiv \exp[\phi(t)] - 1$, which shows that higher temperatures are more heavily damped and thus the peak in the scattering rates shifts to lower frequencies.

With these scattering rates as input, we solve the ME to calculate steady-state exciton populations, N_x, as a function of detuning. We adopt the bath temperature $T = 4\,$K, since it yields the larger asymmetry of rates, and choose a fairly large pump value $\eta_c = 0.3g'$. In order to clearly demonstrate the dominant influence of phonon scattering, exciton populations calculated with the scattering term [Eq. (7)] included are compared against those with phonon scattering turned off; g takes the value of g' in the latter case. The comparison is made in Fig. 3. The figure shows the exciton population passing through a peak as a function of $\omega_L - \omega_x$, more or less in line with the peak in the scattering rates. Most notably, large population inversions are obtained with the cavity blue-shifted from the exciton; this is the configuration that allows phonon scattering between ground- and excited-state branches of the multi-photon ladder of states to excite the exciton, as shown in Fig. 1(d). The reverse process—*cavity feeding*—has been identified in semiconductor cavity-QED studies [12, 20, 22, 23]. Here we see that the phonon-mediated scattering process described by $\Gamma_{\rm ph}^{\sigma^+a}$ can create large population inversions. We stress that the mechanism is quite different to the one reported in Refs. [6] and [4], and the process considerably more efficient. Not only do we see pronounced inversion in the presence of phonon scattering, with $N_x > 0.9$ at cavity detuning $\Delta_{cx} = 1.6\,$meV in Fig. 3, but also significant inversion over a broad detuning range.

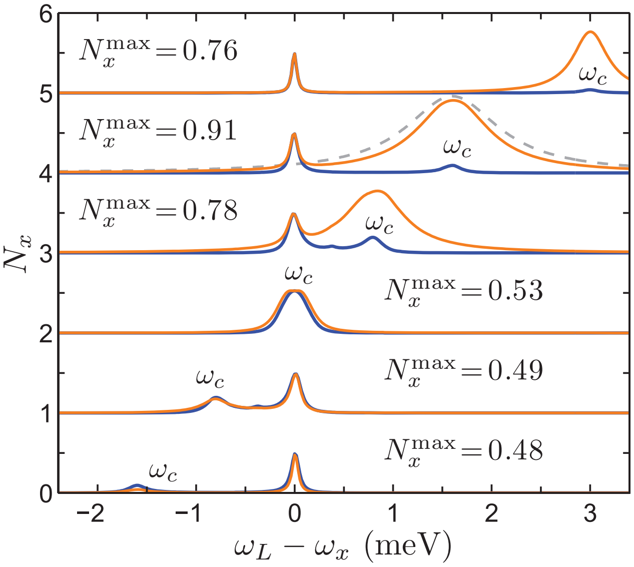

FIG. 3: (Color online) Steady-state exciton population as a function of laser frequency for pump rate $\eta_c = 0.3$ meV and cavity-exciton detunnings $\Delta_{cx} = -1.6$, -0.8, 0, 0.8, 1.6, and 3.0 meV (lower to upper). The blue (dark) curves show the population without phonon scattering while the orange (light) curves include phonon scattering. Each curve is labeled by the peak population with phonon scattering included; the bare cavity resonance is indicated by the vertical magenta line. The dashed line ($\Delta_{cx} = 1.6\,$meV) shows results with the JC term ($\hbar g' X_g$) omitted from the polaron-transformed Hamiltonian [coupled harmonic ladders, cf. Fig. 1(d)].

Phonon-mediated population inversion is unique to the solid state environment where it may allow for cavity-pumped single exciton lasing. It is important to note that these predictions are maintained when the full non-

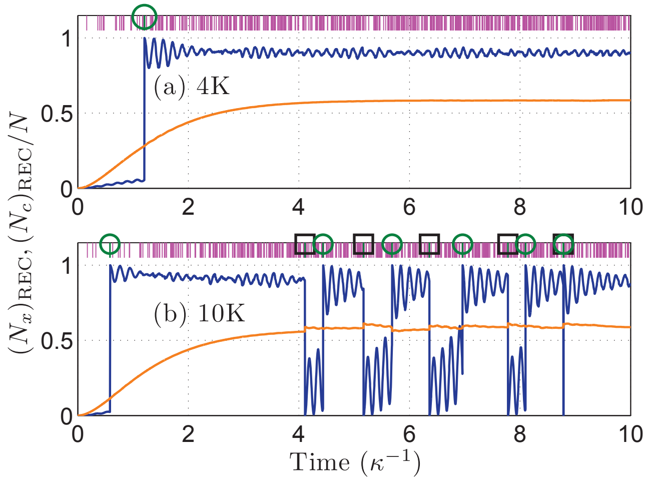

FIG. 4: (Color online) Examples of quantum trajectories at (a) 4 K and (b) 10 K, for optimal detuning, $\Delta_{cx} = 1.6\,$meV, and other parameters as in Fig. 2. Orange (light) lines display the photon number expectation $(N_c)_{\rm REC}/N = \langle a^\dagger a\rangle_{\rm REC}/N$ (truncation at $N = 60$) and blue (dark) lines the exciton expectation $(N_x)_{\rm REC} = \langle\sigma^+\sigma^-\rangle_{\rm REC}$. The expectations are *conditioned* upon the record of quantum jumps: either photon decay (magenta lines) or phonon-mediated scattering [green circles (black squares) for scattering at rate $\Gamma_{\rm ph}^{\sigma^+ a}$ ($\Gamma_{\rm ph}^{a^\dagger\sigma^-}$)].

Lindblad ME is used [14].

At the optimal cavity detuning near $\Delta_{cx} = 1.6\,$meV, the exciton population is greater than 0.9; even higher numbers result at higher pump rates. As indicated above [cf. Fig. 1(d)], the mechanism underlying this remarkable inversion is described in a simplest model by electron-phonon scattering between a pair of cavity multi-photon ladders—the first coordinated with the ground state of the exciton and the second the excited state. The model neglects the JC interaction term ($\hbar g' X_g$) in polaron-transformed Hamiltonian [Eq. (4)]. To test it, we also carried out calculations with the JC term omitted; our results for $\Delta_{cx} = 1.6\,$meV appear as the dashed curve in Fig. 3. They confirm the qualitative correctness of the model, with large population inversions near the cavity frequency reproduced; although, as one would expect, the exciton resonance is completely missed.

Finally, two sample quantum trajectory simulations [24] are presented in Fig. 4 to provide insight into changes brought by the neglected JC interaction term. For the optimum detuning of $\Delta_{cx} = 1.6$ meV, we contrast the phonon scattering dynamic at temperatures of 4 K and 10 K. Short vertical magenta lines signal cavity photon jumps, while green circles and black squares identify the jumps associated with phonon scattering—photon annihilation accompanied by exciton exitation (green circles) and photon creation accompanied by exciton deexcitation (black squares). Phonon scattering quickly (within a cavity lifetime) excites the exciton. The excitation is maintained over a relatively long time at 4 K, eventually being lost primarily through radiative decay; the low radiative decay rate means no such γ-jump occurs in Fig. 4. With the temperature increased to 10 K, the reverse phonon scattering process primarily deexcites the exciton at a higher rate, and populations are reduced. In the present case, increasing the temperature from 4 K to 10 K reduces the inversion from 0.9 to approximately 0.8. The effect of the JC interaction term is to produce the oscillations in Fig. 4, hardly altering the pattern of quantum jumps but reducing the mean population a little (c.f. the dashed curve in Fig. 3).

Conclusion.—We have reported a fundamentally new way of creating pronounced exciton inversions in semiconductor QD-cavity systems. The mechanism exploits a highly efficient phonon-mediated scattering process that destroys cavity photons while creating excited excitons; the reverse process takes place at a much reduced rate in a low temperature bath. At a phonon bath temperature of 4 K, exciton populations greater than 0.9 are easily achievable.

This work was supported by the National Sciences and Engineering Research Council of Canada and the Marsden Fund of the Royal Society of New Zealand.

---

[*] Electronic address: shughes@physics.queensu.ca

[1] See, e.g., P. W. Milloni and J. H. Eberly, *Laser Physics* (Wiley, New York, 2009).
[2] M. Mu and C. M. Savage, Phys. Rev. A **46**, 5944 (1992).
[3] J. McKeever, A. Boca, A. D. Boozer, J. R. Buck, and H. J. Kimble, Nature **425**, 268 (2003).
[4] S. Hughes and H. J. Carmichael, Phys. Rev. Lett. **107**, 193601 (2011).
[5] P. J. Leek, S. Filipp, P. Maurer, M. Baur, R. Bianchetti, J. M. Fink, M. Göppl, L. Steffen, and A. Wallraff, Phys. Rev. B **79**, 180511(R) (2009).
[6] C. M. Savage, Phys. Rev. Lett. **60**, 1828 (1988).
[7] M. Florescu and S. John, Phys. Rev. A **64**, 033801 (2001)
[8] See, e.g., K. Hennessy, A. Badolato, M. Winger, D. Gerace, M. Atatüre, S. Gulde, S. Fält, E. L. Hu and A. Imamoğlu, Nature 445, 896 (2007); M. Nomura, N. Kumagai, S. Iwamoto, Y. Ota, and Y. Arakawa, Nature Phys. **6**, 279 (2010).
[9] L. Besombes, K. Kheng, L. Marsal, and H. Mariette, Phys. Rev. B **63**, 155307 (2001).
[10] A. J. Ramsay, A. V. Gopal, E. M. Gauger, A. Nazir, B. W. Lovett, A. M. Fox, and M. S. Skolnick, Phys. Rev. Lett. **104**, 017402 (2010).
[11] S. M. Ulrich, S. Ates, S. Reitzenstein, A. Löffler, A. Forchel and P. Michler, Phys. Rev. Lett. **106**, 247402 (2011).
[12] C. Roy and S. Hughes, Phys. Rev. Lett. **106**, 247403 (2011).
[13] J. Förstner, C. Weber, J. Danckwerts, and A. Knorr, Phys. Rev. Lett. **91**, 127401, 2003.
[14] C. Roy and S. Hughes, Phys. Rev. X **1**, 021009 (2011).
[15] S. Hughes and H. Kamada, Phys. Rev. B **70**, 195313

(2004).
[16] G. D. Mahan, *Many-Particle Physics*, Plenum, New York, 1990.
[17] I. Wilson-Rae and A. Imamoğlu, Phys. Rev. B **65**, 235311 (2002).
[18] B. Krummheuer, V. M. Axt, and T. Kuhn, Phys. Rev. B **65**, 195313 (2002).
[19] D. P. S. McCutcheon and A. Nazir, New Jour. Phys. **12**, 113042 (2010).
[20] S. Hughes, P. Yao, F. Milde, A. Knorr, D. Dalacu, K. Mnaymneh, V. Sazonova, P. J. Poole, G. C. Aers, J. Lapointe, R. Cheriton and R. L. Williams, Phys. Rev. B **83**, 165313 (2011).
[21] T. Takagahara, Phys. Rev. B **60**, 2638 (1999).
[22] U. Hohenester, Phys. Rev. B **81**, 155303 (2010).
[23] M. Calic, P. Gallo, M. Felici, K. A. Atlasov, B. Dwir, A. Rudra, G. Biasiol, L. Sorba, G. Tarel, V. Savona, and E. Kapon, Phys. Rev. Lett. **106**, 227402 (2011).
[24] See, e.g., J. Dalibard, Y. Castin, and K. Mølmer, Phys. Rev. Lett. **68**, 580 (1992); L. Tian and H. J. Carmichael, Phys. Rev. A **46**, R6801 (1992).